

Deterministic and stochastic behaviour of non-Brownian spheres in sheared suspensions

By GERMAN DRAZER¹, JOEL KOPLIK¹,
BORIS KHUSID² AND ANDREAS ACRIVOS¹

¹The Levich Institute, T-1M, The City College of the City University of New York,
New York, NY 10031, USA

²Department of Mechanical Engineering, New Jersey Institute of Technology,
University Heights, Newark, New Jersey 07102

(Received 28 October 2018)

The dynamics of macroscopically homogeneous sheared suspensions of neutrally buoyant, non-Brownian spheres is investigated in the limit of vanishingly small Reynolds numbers using Stokesian dynamics. We show that the complex dynamics of sheared suspensions can be characterized as a chaotic motion in phase space and determine the dependence of the largest Lyapunov exponent on the volume fraction ϕ . We also offer evidence that the chaotic motion is responsible for the loss of memory in the evolution of the system and demonstrate this loss of correlation in phase space. The loss of memory at the microscopic level of individual particles is also shown in terms of the autocorrelation functions for the two transverse velocity components. Moreover, a negative correlation in the transverse particle velocities is seen to exist at the lower concentrations, an effect which we explain on the basis of the dynamics of two isolated spheres undergoing simple shear. In addition, we calculate the probability distribution function of the velocity fluctuations and observe, with increasing ϕ , a transition from exponential to Gaussian distributions.

The simulations include a non-hydrodynamic repulsive interaction between the spheres which qualitatively models the effects of surface roughness and other irreversible effects,

such as residual Brownian displacements, that become particularly important whenever pairs of spheres are nearly touching. We investigate the effects of such a non-hydrodynamic interparticle force on the scaling of the particle tracer diffusion coefficient D for very dilute suspensions, and show that, when this force is very short-ranged, D becomes proportional to ϕ^2 as $\phi \rightarrow 0$. In contrast, when the range of the non-hydrodynamic interaction is increased, we observe a crossover in the dependence of D on ϕ , from ϕ^2 to ϕ as $\phi \rightarrow 0$.

1. Introduction

The phenomenon of shear-induced particle diffusion in suspensions at vanishingly small Reynolds number has been studied extensively since the work of Eckstein *et al.* (1977), where it was first suggested that a shear flow causes the particles to execute random migrations across the streamlines of the ambient flow producing an effect akin to dispersion. This hypothesis of a self-diffusive motion arising from purely viscous hydrodynamic interactions between particles has already received considerably experimental support (Eckstein *et al.* 1977; Leighton & Acrivos 1987; Breedveld *et al.* 1998, 2001*b,a*). Moreover, as pointed out by Breedveld *et al.* (2001*b*), the origin of this diffusive behaviour is clearly different from the more familiar Brownian diffusion in colloidal suspensions caused by thermal fluctuations, as well as turbulent diffusion driven by inertial effects, in that this shear-induced diffusion is due only to the hydrodynamic interactions between the particles comprising the suspension. Since, in principle, these interactions constitute a deterministic process, the question arises as to whether and how it can also be viewed as a diffusion process. To address this question, it is generally assumed that the arrangement of neighboring suspended spheres leads to a time-dependent random event

(Eckstein *et al.* 1977) in that, upon *collision* with their closest neighbors, the spheres will suffer many successive random displacements ultimately leading to a random walk (Leighton & Acrivos 1987; Zarraga & Leighton 1999). Underlying this description is the fundamental assumption that collisions between spheres eventually become statistically independent. Although many theoretical studies have made this strong assumption in order to calculate the diffusivity of very dilute sheared suspensions from the displacement produced by a single collision and then averaging over all initial configurations of the colliding spheres (Acrivos *et al.* 1992; Wang *et al.* 1996, 1998; da Cunha & Hinch 1996), the complex dynamics of suspensions undergoing shear, leading to the loss of correlations in the particle motions, has not been investigated thus far in much detail.

It is the purpose of the first part of this work to pursue the recent suggestion made by Marchioro & Acrivos (2001) that the chaotic evolution of sheared suspensions is responsible for the *loss of memory* referred to above, and to demonstrate, via numerical simulations, that the evolution of the system in phase space is indeed chaotic. Recall that chaotic dynamics is characterized by the sensitivity of the system to initial conditions, as evidenced by the exponential growth of the separation distance in phase space of two initially neighboring trajectories, and that a standard measure of this sensitivity is the largest Lyapunov exponent (LLE), which gives the average rate of this separation distance (Baker & Gollub 1990, p. 85). We shall therefore investigate the LLE as a function of the volume fraction ϕ of the suspensions. We shall also show that the system loses the memory of its initial state and that its evolution is asymptotically diffusive. The loss of memory at the level of a single sphere will also be discussed in terms of the autocorrelation functions of the two transverse velocity components, and we will show that, as the concentration is increased and collisions between spheres become more

frequent, the time scale over which the particle transverse velocities remain correlated is shortened.

Before proceeding, it is instructive to consider the motion of a tracer sphere subject to purely hydrodynamic interactions with the other spheres in the suspension. As is well-known, and as a direct consequence of the linearity of the equations of motion at zero Reynolds number, in any encounter between two perfectly smooth spheres neither sphere experiences a net lateral displacement, although both may suffer large transient displacements from their original streamlines (Leal 1992, p. 257). Therefore, for the tracer to experience a net displacement leading to diffusive motion it is necessary that it interact with at least two other spheres. Since the rate of simultaneous interactions of a tracer sphere with two other spheres is proportional to $\gamma\phi^2$ as $\phi \rightarrow 0$, where γ is the shear rate, and since the magnitude of each displacement is proportional to the particle radius a , the self-diffusion coefficient should be proportional to $\gamma\phi^2a^2$, in the limit of very dilute suspensions (Leighton & Acrivos 1987). The experimental results by Leighton & Acrivos (1987) observe this scaling for volume fractions $0.05 < \phi < 0.40$. However, in any real experiment, suspended particles are not perfectly spherical and, as the separation between two colliding particles can be very small (less than 10^{-4} of a particle radius (da Cunha & Hinch 1996)), even very small asperities might play a significant role during encounters between a pair of spheres. In experiments performed by Rampall *et al.* (1997) a roughness of order 10^{-3} particle radii was found, and the effect of the asperities on the trajectories of nearly touching spheres during a collision was determined. In this situation, the interaction of the tracer particle with another sphere *will* lead to a net displacement of the tracer from its original streamline, and therefore, since the rate of interactions with another sphere is proportional to $\gamma\phi$, the diffusion coefficient is expected to scale as $\gamma\phi a^2$ as $\phi \rightarrow 0$. This linear dependence of the diffusion coefficient on ϕ was observed in

experiments performed by Phan & Leighton (1999) and by Zarraga & Leighton (1999). On the other hand, thus far, the numerical simulations of sheared suspensions have not been extended to low enough values of ϕ where one or the other of these two regimes for the diffusivity would be expected to apply.

In this work, we shall therefore investigate the scaling of the diffusion coefficient by performing simulations down to values of ϕ as low as 0.03. The effect of surface roughness and other possible non-hydrodynamic forces, such as residual Brownian forces, will be qualitatively modelled by introducing a short-ranged repulsive force between the spheres. This is similar to the approach taken by da Cunha & Hinch (1996) and by Zarraga & Leighton (1999), where the surface roughness was modelled as a normal force that prevents the particles from coming closer than a certain fixed distance. As discussed above, the contribution to the diffusive motion of the spheres due to binary collisions clearly depends on the magnitude and range of the interparticle force, in that for a weak force, a $\gamma\phi^2a^2$ regime for the diffusivity would be expected. However, since at low enough concentrations, the linear regime should eventually become dominant no matter how small the effect of the interparticle force, we shall investigate this transition from a quadratic to a linear dependence of the diffusivity on ϕ as $\phi \rightarrow 0$. As a preliminary, in §2.1 we shall discuss the effects of such a non-hydrodynamic interparticle force on the microscopic structure of the suspension, and in particular its dependence on the strength and the range of this force.

2. Simulation method: Stokesian dynamics

We consider suspensions of non-Brownian particles undergoing shear using the method of Stokesian Dynamics which was specifically developed for dynamically simulating the behaviour of many particles suspended in a fluid (Brady & Bossis 1984). A detailed de-

scription of the method is given in a review by Brady & Bossis (1988), hence only a brief discussion is presented here. The method accounts for both hydrodynamic and non-hydrodynamic forces between particles. Hydrodynamic forces are computed for spherical particles undergoing simple shear, characterized by a shear rate γ , in the limit of zero Reynolds number. In simulating the behaviour of infinite suspensions, periodic boundary conditions in all direction are imposed, using an adapted version of the Lees-Edwards boundary condition in the direction of the shear (Allen & Tildesley 1987, p. 242)(Brady & Bossis 1985). The volume V of the cubic cell containing a fixed number of spheres N is related to the volume fraction ϕ by $\phi = (4\pi a^3/3)N/V$. Interactions between particles more than a cell apart from each other cannot be neglected, due to the long-range character of the hydrodynamic forces, and a lattice sum of the interactions, using the Ewald method, is implemented (Brady *et al.* 1988).

A typical simulation here consists of $N = 64$ particles sheared over a period of time $t \sim 100\gamma^{-1}$. The results are averaged over $N_c \sim 100$ different initial configurations using the random-phase average method proposed by Marchioro & Acrivos (2001), in order to avoid spurious time-periodic fluctuations induced by the time-dependent shape of the simulation cell. Each initial configuration corresponds to a random distribution of non-overlapping spheres in the simulation cell.

In what follows, we shall express all the variables in dimensionless units, using the radius of the spheres a as the characteristic length and γ^{-1} as the characteristic time.

2.1. *Non-hydrodynamic interparticle force*

In a suspension of non-Brownian spherical particles undergoing shear at zero Reynolds number, the separation between spheres can be very small (less than 10^{-4} of their radius). In this situation, the effects of surface roughness or small Brownian displacements cannot be neglected and a short-ranged, repulsive force is usually introduced between the spheres

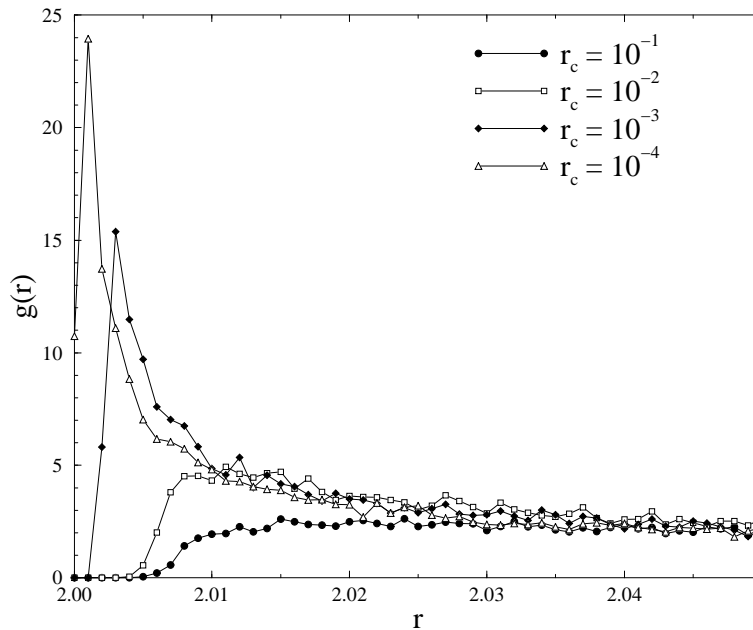


FIGURE 1. First peak of the pair distribution function $g(r)$ for different values of r_c , the characteristic range of the interparticle force. The position of the peak indicates that, as the range of the repulsive force increases, so does the minimum separation between particles. The simulations are for $\phi = 0.10$, $N = 64$, $F_0 = 1.0$, and $N_c = 100$. $g(r)$ is measured after each initial random distribution of spheres is sheared for $t \sim 50$ and steady state was reached.

to qualitatively model the behaviour of real systems. The introduction of such a force has the further numerical advantage of preventing overlaps between the spheres.

In this work we used the expression for the repulsive interparticle force, already well-tested in the context of Stokesian dynamics,

$$\mathbf{F}_{\alpha\beta} = \frac{F_0}{r_c} \frac{e^{-\epsilon/r_c}}{1 - e^{-\epsilon/r_c}} \mathbf{e}_{\alpha\beta}, \quad (2.1)$$

where $6\pi\mu a^2\gamma\mathbf{F}_{\alpha\beta}$, with μ being the viscosity of the suspending liquid, is the force exerted on sphere α by sphere β , F_0 is a dimensionless coefficient reflecting the magnitude of this force, r_c is the characteristic range of the force, ϵ is the distance of closest approach

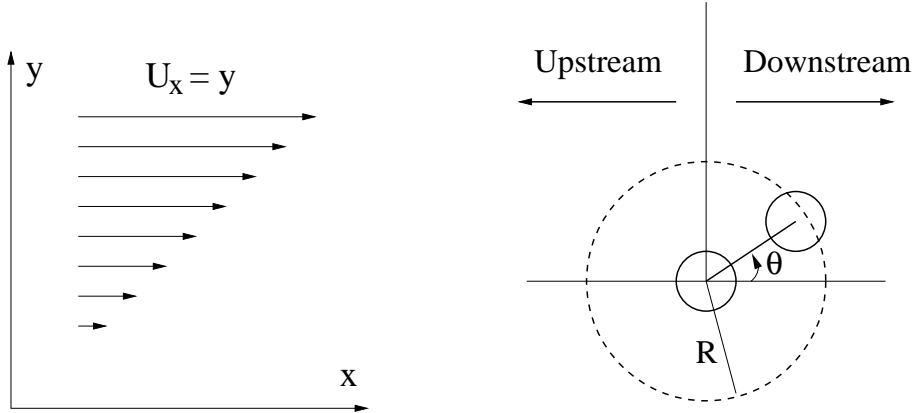


FIGURE 2. Diagram of a pair of spheres oriented with an angle θ measured from the downstream side of the reference sphere. Down and upstream sides of the reference sphere as well as the distance R defining particle pairs are shown.

between the surfaces of the two spheres divided by a , and $\mathbf{e}_{\alpha\beta}$ is the unit vector connecting their centres pointing from β to α .

The magnitude and range of the interparticle force affect the microstructure of the suspension (Brady & Morris 1997). As mentioned earlier, colliding spheres in a shear flow almost touch one another, with the actual minimum separation distance strongly dependent on the repulsion between them. Following Bossis & Brady (1984) we show this effect in figure 1 in terms of the pair distribution function $g(r)$, defined as the probability of finding the centre of a second particle at a distance $r = |\mathbf{r}|$ given that there exists a sphere with its origin at $\mathbf{r} = 0$. We see that the minimum separation, and therefore the first peak in $g(r)$, is strongly affected by the range of the interparticle force in that, as r_c increases, the minimum separation between neighboring particles also increases.

It is also known that the presence of a repulsive force breaks the angular symmetry of the microstructure and, in particular, that it destroys the fore-aft symmetry of the particle trajectories in a simple shear flow (Bossis & Brady 1984; Dratler & Schowalter 1996). Specifically, again following Bossis & Brady (1984), let us consider the angular orientation of *pairs* formed by spheres closer than a certain distance R , and let us define

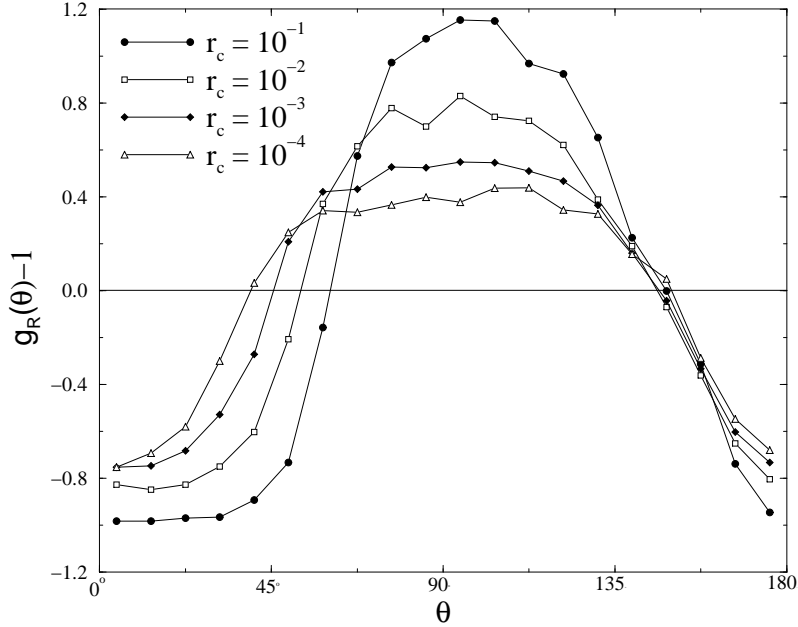


FIGURE 3. Normalized angular distribution function $g_R(\theta)$ for pairs of particles. The distance between the particles is $2 < r < 2.1$ ($R = 2.1$). Different curves correspond to different values of the interparticle force range r_c . All simulation were performed with $N = 64$, $N_c = 100$, $F_0 = 1.0$ and $\phi = 0.10$.

the probability distribution $g_R(\theta)$ as the probability density of finding a pair having a given orientation angle θ (c. f. figure 2). It is clear that, as already shown by Bossis & Brady (1984), particle pairs would be expected to spend more time oriented on the upstream side, where the repulsive force is balanced by the shear forces pushing the two particles together, implying that the probability of finding a pair oriented upstream, $90^\circ < \theta < 180^\circ$, would be higher than in the downstream range, $0^\circ < \theta < 90^\circ$. This is borne out by figure 3 which shows that the pair distribution function becomes increasingly more asymmetric, favoring the upstream orientation of particle pairs, as the range of the interparticle force is increased.

In addition to the microscopic effects mentioned above, the interparticle force also affects macroscopic measurable quantities, as we shall discuss in the following sections.

3. Chaotic motion and time-reversibility

As already mentioned in the introduction, the question as to whether and how diffusive-like transport arises in a suspension of non-Brownian particles undergoing shear has been investigated since the original work by Eckstein *et al.* (1977). Experimental evidence strongly suggests that even with vanishingly small inertia effects (zero Reynolds number) and negligible Brownian and non-hydrodynamic forces, sheared suspensions exhibit diffusive behaviour (Leighton & Acrivos 1987; Breedveld *et al.* 1998, 2001*b,a*).

In an ideal case, where only hydrodynamic forces are present and the Reynolds number is exactly zero, the motion of the particles is deterministic and reversible due to the linearity of the governing flow equations, thereby implying that, upon reversing the direction of flow, the particles should retrace their trajectories. However, in any physical experiment, there exists inherent slight irreversible effects at the microscopic level, such as residual Brownian motion and surface-roughness effects, which, as is usually the case in dynamical systems, can have a strong impact on macroscopic measurable quantities. As an example, let us consider again the loss of fore-aft symmetry in sheared suspensions.

It can be shown, based upon the reversibility of Stokes flow, that the pair distribution function of sheared suspension of perfect spheres should have fore-aft symmetry. On the other hand, since the original work by Gadala-Maria & Acrivos (1980), there exists strong experimental evidence that, even at vanishingly small Reynolds numbers and Brownian force effects, sheared suspensions develop an anisotropic structure resulting in the loss of fore-aft symmetry (Parisi & Gadala-Maria 1987; Rampall *et al.* 1997). This broken symmetry has been attributed to surface-roughness effects. As mentioned in

§ 2.1 the minimum separation between two colliding spheres in a shear flow can be less than 10^{-4} of their radius, so that even a small surface roughness can have an important influence in this case (da Cunha & Hinch 1996). Thus, small irreversible effects related to surface roughness, which is present at microscopic scales, have a measurable impact on the macroscopic structure of the suspension and correspondingly on related macroscopic quantities such as the normal stress difference in sheared suspensions.

Thus far we have discussed the microscopic origin of irreversibility and its manifestation in macroscopic quantities which provides a microscopic basis for the existence of an intrinsically irreversible macroscopic description as given by the diffusion equation. But, the basic assumption underlying the derivation of such an equation and, in particular, the validity of a statistical description of the system based on the randomness of the microscopic motion of the particles, is in need of further discussion. Recall that, in the calculation of the diffusivity in very dilute sheared suspensions, it is generally assumed that successive collisions between spheres are statistically independent, sometimes referred to as *molecular chaos* (Acrivos *et al.* 1992; Wang *et al.* 1996, 1998; da Cunha & Hinch 1996). Furthermore, it has been suggested that a close connection exists between *molecular chaos* and dynamical chaos, according to which stochastic-like behaviour is possible even for deterministic mechanical systems (e. g. Gaspard (1998), p. 225; Dorfman (1998).) In fact, even low-dimensional deterministic dynamical systems are known to give rise to diffusive transport (usually named *deterministic diffusion* (Gaspard 1998, p. 293)). Chaotic systems have the property that any small perturbation in the state of the system will grow exponentially in time, to the point where the evolution can no longer be accurately predicted. But, although the hypothesis of chaotic motion as the basic mechanism responsible for this *loss of memory* and for that matter, as the cause of the phenomenon of shear induced diffusion, has been suggested in the context of sheared

suspensions by Marchioro & Acrivos (2001) and has been supported by their numerical simulations showing irreversible behaviour upon reversal in the direction of the shear, to-date the presence of chaos in a sheared suspension has not been examined. We shall therefore numerically investigate the presence of chaotic motion in sheared suspensions by evaluating the largest Lyapunov exponent which is a standard measure of chaoticity (Schuster 1989, p. 24).

It is worth mentioning here that we do not wish to imply that diffusive motion cannot possibly operate in the purely hydrodynamic case, and that diffusion owes its existence to the unavoidable presence of small microscopic irreversible forces. In fact, the presence of chaotic motion, which we shall presently demonstrate, strongly suggests that, even in the absence of such effects, diffusive behaviour should still arise due to the loss of correlation in the particle motions.

3.1. *Largest Lyapunov exponent*

In a sheared suspension at zero Reynolds number, the state of the system is fully determined by the coordinates of all the particles and, therefore, a sheared suspension consisting of N particles can be considered as a dynamical system in a $3N$ -dimensional phase space. A point of this phase space $\mathbf{\Gamma}$ is given by $3N$ particle coordinates and the Lyapunov exponents measure the average rate of separation of two initially neighboring trajectories in phase space. Thus, given two states of the system separated a small distance $d(0)$ in phase space, the largest Lyapunov exponent (LLE) for that state is formally defined as

$$\lambda = \lim_{t \rightarrow \infty} \lim_{d(0) \rightarrow 0} \left[\frac{1}{t} \frac{d(t)}{d(0)} \right], \quad (3.1)$$

with $d(t)$ being the separation distance in phase space at time t , which controls the exponential divergence of initially close trajectories.

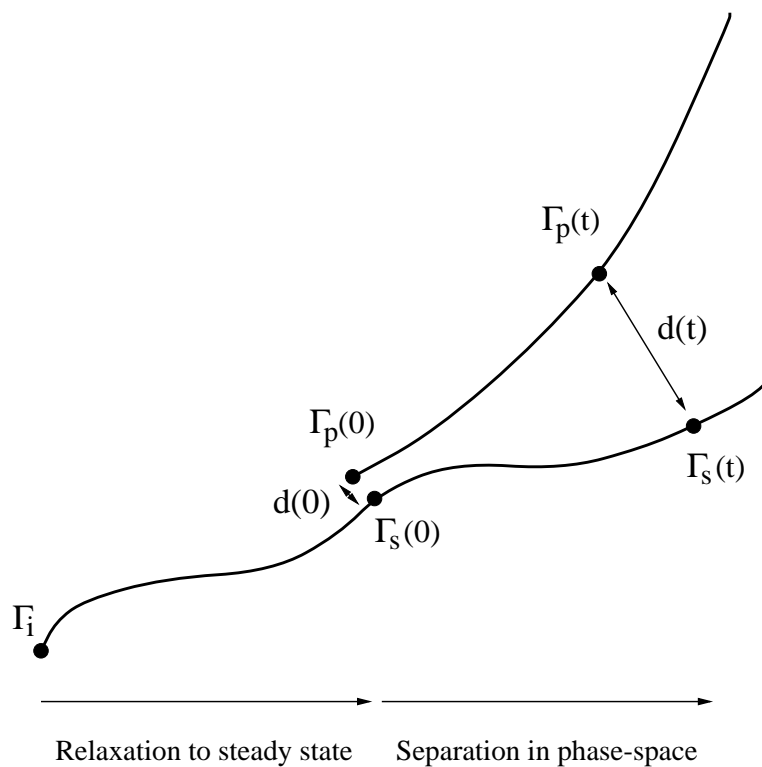


FIGURE 4. Schematic representation of the generation of initially close trajectories in a stationary state. Starting from a random configuration of hard-spheres Γ_i we follow the evolution of the system towards steady state. Once in steady state, we generate a slightly perturbed state Γ_p by adding a small random displacement to each particle. The initial separation in phase space is $d(0)$. Then we follow the evolution of the two systems by computing the distance at each time $d(t)$.

In order to obtain a numerical estimate of the LLE for the steady state of a sheared suspension, we compute the ensemble averaged LLE used in ergodic systems (Gaspard 1998, p. 144, 247) by generating a number N_c of initial configurations $\Gamma_s(0)$ in a steady state flow, starting from a random configuration Γ_i of spheres and evolving the system for a sufficiently long time (typically for strains $t \sim 50$). For each of these configurations we then introduce a slightly perturbed state $\Gamma_p(0)$, by adding a random displacement \bar{d} to $\Gamma_s(0)$ † (see figure 4).

† In order to generate a random perturbation in phase space \bar{d} , with constant magnitude $|\bar{d}| = d(0)$, we initially construct a $3N$ -dimensional vector ξ , where each component ξ_i is a

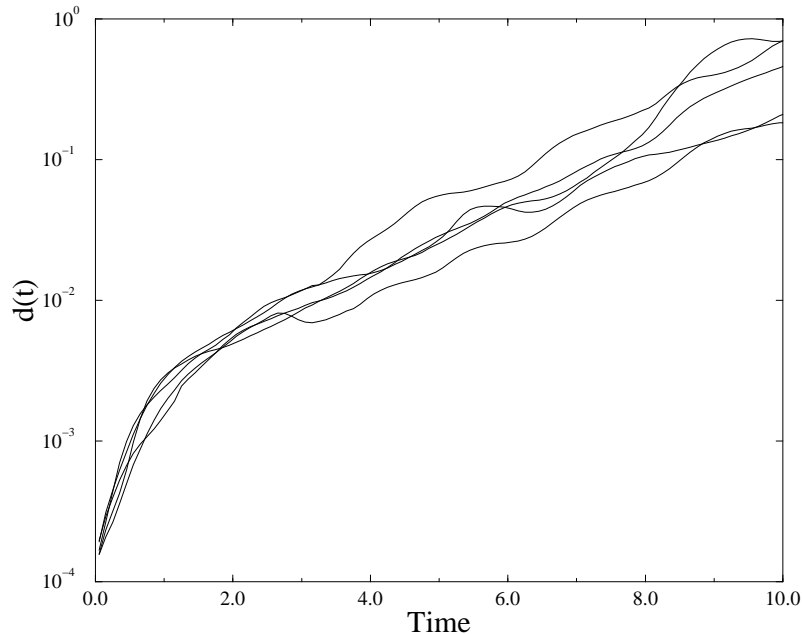


FIGURE 5. Separation of initially close trajectories in phase space $d(t)$ for different initial states of the unperturbed system. The results correspond to simulations with $N = 64$, $F_0 = 1.0$, $r_c = 10^{-4}$, and $\phi = 0.35$.

Following the evolution of these two independent systems we can compute a distance in phase space given by,

$$d(t) = \|\Gamma_s(t) - \Gamma_p(t)\| = \left(\sum_{i=1}^N [\mathbf{x}_s^i(t) - \mathbf{x}_p^i(t)]^2 \right)^{\frac{1}{2}} \quad (3.2)$$

where the indices s and p refer to the unperturbed and perturbed initial states of the two systems[†] (see figure 4). To be sure, for a single realization, $d(t)$ will depend on both initial states $\Gamma_s(0)$ and $\Gamma_p(0)$, but, after some transient behaviour, we should certainly expect random variable with uniform distribution in the range $-1 < \xi_i < 1$. Then, we renormalize this vector to obtain the desired initial magnitude of the perturbation, $\bar{d} = \bar{\xi}(d(0)/|\bar{\xi}|)$. Thus, a random displacement \bar{d} in phase space corresponds, on average, to a random perturbation, of order $d(0)/\sqrt{N}$, to the position of each particle.

[†] Let us mention that, even though the affine shearing motion of the spheres is not removed

an exponential separation with large fluctuations due to the details of the dynamics of the system. This is illustrated in figure 5. In order to compute the LLE accurately, we therefore first average over N_c different initial conditions in phase space, then take the logarithm of the mean exponential separation,

$$\Delta_\Gamma(t) = \ln(\langle d(t) \rangle_\Gamma) = \ln\left(\frac{1}{N_c} \sum_{k=1}^{N_c} \{d(t)\}_k\right) \quad (3.3)$$

and identify λ_Γ (the largest Lyapunov exponent) as the slope of $\Delta_\Gamma(t)$ in the region of its linear growth †.

Analogously, we can define a distance in the space of the transverse velocity components of all the particles,

$$\Delta_v(t) = \ln\left[\frac{1}{N_c} \sum_{k=1}^{N_c} \left\{ \left(\sum_{i=1}^N [\mathbf{v}_s^i(t) - \mathbf{v}_p^i(t)]^2 \right)^{\frac{1}{2}} \right\}_k\right] \quad (3.4)$$

However, as $d(t)$ grows exponentially, so does a generic projection in phase space (or a distance measured with any particular metric). Moreover, since the separation is dominated by the exponential growth with the LLE, and the velocity is the derivative of the and its contribution dominates the initial growth of the separation distance in phase space, the exponential growth should eventually become dominant at long times.

† The method used in this work to compute the largest Lyapunov exponent differs from that described by Benettin *et al.* (1976) and used frequently. Instead of averaging over different realizations (ensemble average), Benettin *et al.* (1976) reset the distance between trajectories to the initial value after fixed intervals of time τ and compute the Lyapunov exponent from the average distance reached before the rescaling procedure (time average). However, both methods should give the same value of λ if the system is ergodic, because in that case, the time-average of any dynamical quantity is equal to its ensemble average over a large number of realizations N_c Eckmann & Ruelle (1985). The main advantage of our method is that it allows us to compute the evolution of all the initial configurations simultaneously, which reduces the computational time enormously, as compared to a single very long simulation, when the computations are performed using a cluster of processors.

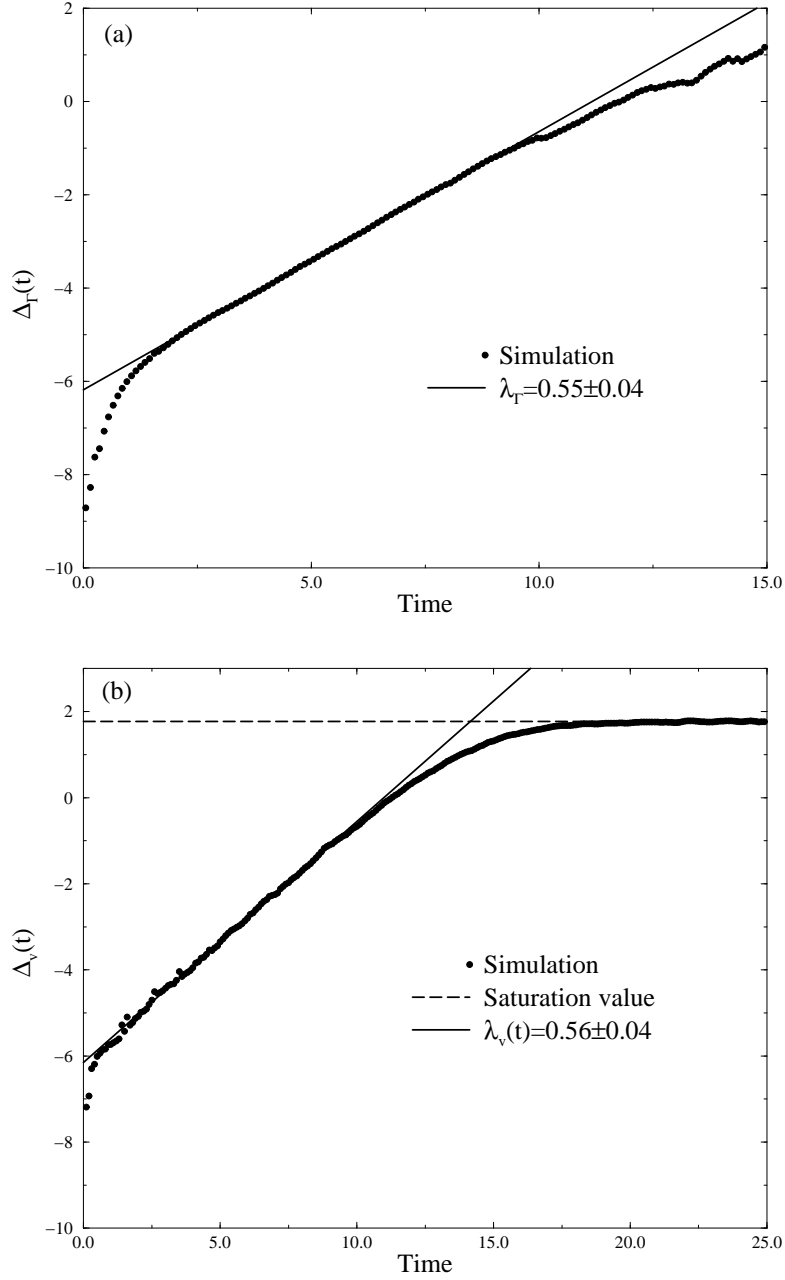


FIGURE 6. Separation of initially close trajectories in phase space. (a) Coordinate phase space, (b) Transverse velocity space. The results corresponds to a sheared suspension of $N = 64$ particles, volume fraction $\phi = 0.35$, interparticle force $F_0 = 1.0$, characteristic range $r_c = 10^{-4}$, and $N_c = 100$. The solid line corresponds to a linear fit with (a) $\lambda = 0.55 \pm 0.04$, (b) $\lambda = 0.56 \pm 0.04$. The dashed line in (b) is the asymptotic value of Δ_v as $t \rightarrow \infty$ given by (3.5).

position of the particles, one would expect the Lyapunov exponent λ_v , as obtained from the slope of $\Delta_v(t)$, to be the same as that measured from $\Delta_\Gamma(t)$, i.e. $\lambda = \lambda_\Gamma = \lambda_v$.

In figure 6 we show the time evolution of $\Delta_\Gamma(t)$ and $\Delta_v(t)$ for a sheared suspension with $N = 64$ particles, volume fraction $\phi = 0.35$, interparticle force $F_0 = 1.0$ and characteristic range $r_c = 10^{-4}$. The distance $d(t)$ was averaged over $N_c=100$ different initial conditions. The initial distance in phase space $\mathbf{\Gamma}$ is $d(0) = 10^{-4}$, which corresponds to a random displacement $\sim 10^{-5}$ added to the position of each particle. Simulations using a smaller initial displacement give a similar behaviour with a variation in the measured Lyapunov exponent less than 5%. We also performed simulations with $r_c = 10^{-3}$ as well as with $F_0 = 0.1$, but, in all cases, the variations between the LLE's were within 10%. However, larger changes should be expected in the value of the LLE for larger variations in the range or the strength of the interparticle force. Finally, the Lyapunov exponent calculated from $\Delta_\Gamma(t)$ and from $\Delta_v(t)$ is, as expected, the same, within the error in its determination.

In figure 6 three different regimes can be directly observed, a short initial transient behaviour, a large linear growth corresponding to the exponential divergence in phase space and a deviation from the linear growth at long times, corresponding to an asymptotic saturation in velocity space.

There are two related effects that might cause the short-time transient behaviour. On one hand, many-body nonlinear effects only come into play after at least one collision has taken place, and we can therefore relate the transient time to a characteristic time between collisions. During this initial time the distance grows mainly due to the shear flow imposed to the particles. However, the definition of such a characteristic time is not clear, given the fact that the hydrodynamic forces are long ranged. The experiments of Breedveld *et al.* (2001b) found a similar transition when measuring the diffusivity of the particles. They suggested that this transition might correspond to the deformation,

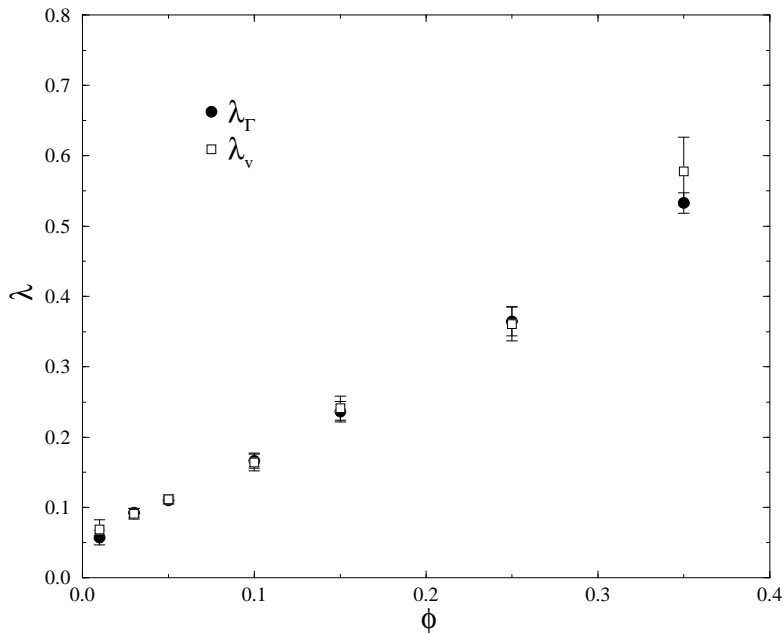


FIGURE 7. Dependence of the Lyapunov exponent on the volume fraction. The results correspond to numerical simulations for $N = 64$, $N_c = 100$, $F_0 = 1.0$ and $r_c = 10^{-4}$. λ_Γ is computed from the separation growth in coordinates phase space, and λ_v using the transverse velocity space.

due to the shear flow, of the initial cloud of particles surrounding a test sphere. In our simulations we found that this transient time decreases with increasing concentration, which is consistent with the suggestion referred to above.

In the simulations it is observed that the distance in the transverse velocity space saturates. This saturation takes place because the definition of the distance in the transverse velocity space does not include the affine motion of the particles, and therefore, two randomly chosen systems in steady state will have a finite mean distance. In fact, the saturation distance can be estimated by assuming that the perturbed system loses memory of its initial unperturbed state. In this case, if we further assume that Δ_v^∞ becomes

$$\Delta_v^\infty = \ln \left[\left\langle \left[N \left\langle (\mathbf{v}_s^i - \mathbf{v}_p^i)^2 \right\rangle_N \right]^{\frac{1}{2}} \right\rangle_\Gamma \right] \approx \ln [2N (\sigma_{vy}^2 + \sigma_{vz}^2)]^{\frac{1}{2}} \quad (3.5)$$

where $\sigma_{v_i}^2$ is the variance in the i -th component of the velocity, the saturation constant can be computed in the steady state, independently of the evolution. For the simulation shown in figure 6, the variances in the velocity components are $\sigma_{v_y}^2 = 0.20$ and $\sigma_{v_z}^2 = 0.07$ respectively, giving a saturation value $\Delta_v^\infty = 1.77$ which is in excellent agreement with the observed saturation distance, as shown by the dashed line in figure 6. On the other hand, as the velocity-space distance saturates, the system loses its memory of the initial state so that the separation in coordinate-phase deviates from the exponential growth, as can be observed in figure 6. In fact, the loss of memory of the initial state of the system leads to an asymptotic diffusive behaviour in phase space.

3.2. Dependence of the Lyapunov exponent on the concentration

We investigated the dependence of the largest Lyapunov exponent on the volume fraction of the suspension. As the concentration increases, the frequency of collisions also increases and we may expect an enlarged sensitivity to the initial conditions. In figure 7 we show the numerical values of the LLE as a function of ϕ . It can be seen that the stochasticity of the system increases with concentration, as measured by λ . An almost linear dependence can be also observed, with the surprising fact that the LLE appears to remain finite as $\phi \rightarrow 0$. We remark parenthetically that, in kinetic theory the Lyapunov exponent can be shown to be a linear function of the frequency of collisions (Gaspard (1998), p. 8; Dorfman (1998)), and that in a sheared suspension, the frequency of collisions is roughly $\nu \sim \phi$. However, due to the long-range interactions between the particles, it is not clear that the same relation between the LLE and ν will continue to apply in the case of sheared suspensions; this then is the main difference between the present situation and kinetic theory, which is based on the existence of short-range interactions between the particles. In fact, the presence of these long-range hydrodynamic forces might be responsible for the curious behavior, seen in figure 7, of λ at small volume fractions. Unfortunately, the

observed initial transient time increases as the concentration becomes smaller, thereby limiting the range of concentrations which we were able to investigate to $\phi > 0.01$. Thus, the functional dependence of the LLE on ϕ in the dilute limit remains an open problem.

4. Transverse velocity autocorrelation function

In the previous section we discussed the global loss of memory of a system when its initial state is slightly perturbed. At the level of individual particles this asymptotic stochastic motion is also present, and could be studied by examining whether the velocity of a particle decorrelates from its initial value. The average correlations between the velocity of a particle at two different times are measured via the velocity autocorrelation function. Here, we consider $K_\alpha(t)$, where α refers to the transverse velocity component being measured

$$\begin{aligned} K_\alpha(t) &= \langle v_\alpha(0)v_\alpha(t) \rangle / \sigma_{v_\alpha}^2 \\ &= \left[\frac{1}{N_c} \sum_{k=1}^{N_c} \left\{ \frac{1}{N} \sum_{i=1}^N v_\alpha^i(0)v_\alpha^i(t) \right\}_k \right] / \left[\frac{1}{N_c} \sum_{k=1}^{N_c} \left\{ \frac{1}{N} \sum_{i=1}^N v_\alpha^i(0)v_\alpha^i(0) \right\}_k \right], \end{aligned} \quad (4.1)$$

and its time integral τ_{v_α}

$$\tau_{v_\alpha} = \frac{1}{\sigma_{v_\alpha}^2} \int_0^\infty dt \langle v_\alpha(0)v_\alpha(t) \rangle = \int_0^\infty dt K_\alpha(t) \quad (4.2)$$

The importance of these functions in computer simulations is well known (Allen & Tildesley 1987, p. 58) and, in particular, the velocity autocorrelation function is related to the diffusion coefficient through,

$$D_{\alpha\alpha} = \int_0^\infty \langle v_\alpha(0)v_\alpha(t) \rangle dt = \sigma_{v_\alpha}^2 \tau_{v_\alpha}. \quad (4.3)$$

This expression has been used in the context of suspensions by Nicolai *et al.* (1995) to determine the diffusivity of sedimenting non-Brownian spheres, and by Marchioro & Acrivos (2001) to measure the shear-induced self-diffusivities.

In figure 8 we show the computed velocity autocorrelation functions for both transverse

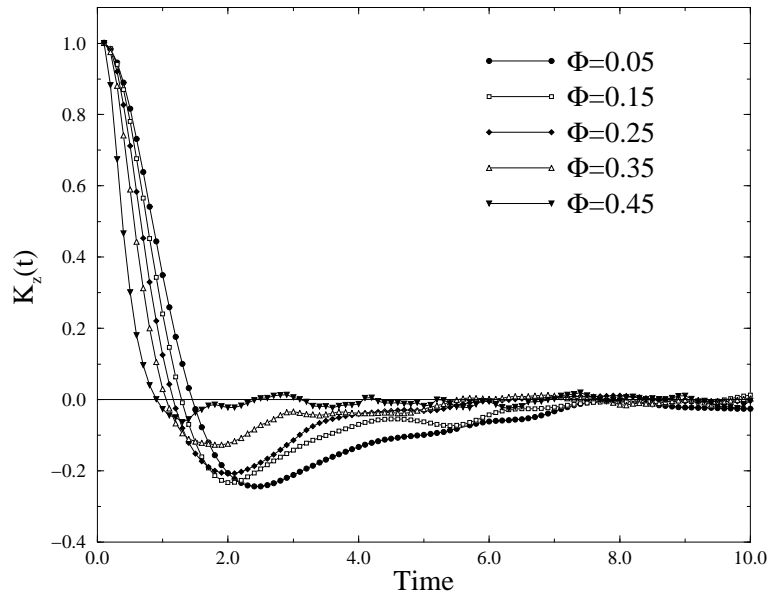
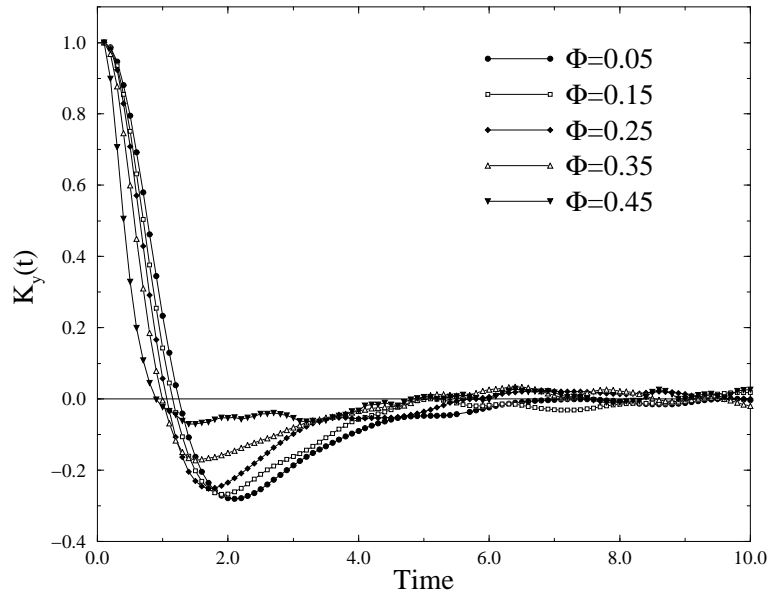


FIGURE 8. Transverse velocity autocorrelation functions in y and z . The simulations are for

$$N = 64, N_c = 100, F_0 = 1.0 \text{ and } r_c = 10^{-4}.$$

velocity components, $K_y(t)$ and $K_z(t)$, for volume fractions ranging between $0.05 < \phi < 0.45$, where y and z are, respectively, along and normal to the plane of shear. In all cases, the velocities become uncorrelated at long times, around $t = 10$ for the lowest volume fraction, and from then on oscillations around zero could be attributed to statistical noise. Thus, for t beyond about 10, the displacement of an individual particle is independent of its displacement at previous times and hence should be describable in terms of a random walk.

It can also be observed that, except at high concentrations ($\phi \approx 0.45$), the autocorrelation function becomes negative over a range of several time units. Let us mention, that a similar behaviour for the velocity autocorrelation function was found in molecular dynamics simulations of simple liquids (Alder & Wainwright 1958; Rahman 1964), and was explained in terms of the backscattering by neighboring particles at high densities (Alder & Wainwright 1967, 1970). In fact, the negative correlation in velocity suggests that, on average, individual particles reverse their velocity, typically after a time interval of order 1 according to our simulations. This result can be understood in terms of the motion of colliding particles in linear shear flow. Specifically, as was already mentioned in the introduction, when two isolated spheres collide, the net displacement in both transverse directions is zero, as a consequence of the reversibility of the creeping flow equations and the symmetry of the problem. However, the instantaneous deviation in the velocity of the spheres during the encounter is not zero and clearly anti-correlated, since the net displacement should integrate to zero. Thus, encounters between two isolated spheres undergoing linear shear flow give rise to a negative correlation in the velocity fluctuations. On the other hand, encounters involving three or more particles will, in general, not be symmetric and the particles will experience a net displacement from their original streamlines (Wang *et al.* 1996). Therefore, in general, the interaction between more

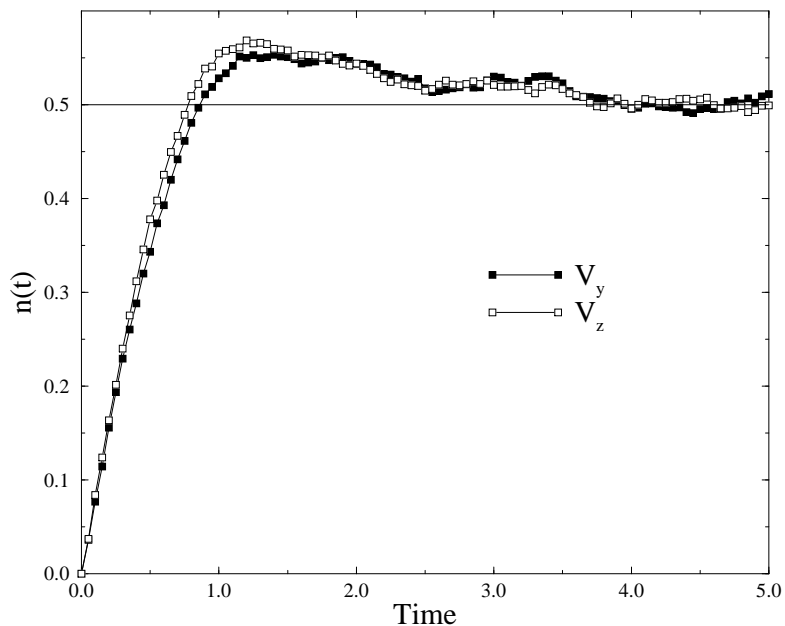


FIGURE 9. Average number of particles with their transverse velocities reversed from their initial direction. Different curves corresponds to different components of the velocity as indicated. The simulations are for $N = 64$, $N_c = 100$, $F_0 = 1.0$, $r_c = 10^{-4}$ and $\phi = 0.35$.

than two particles does not necessarily contribute to a negative autocorrelation in the transverse velocity.

The previous discussion not only explains the observed negative correlation but also the fact that it becomes more pronounced with decreasing volume fraction and that, as $\phi \rightarrow 0$, it seems to converge to an asymptotic function dominated by two-particle encounters.

At high concentrations we see that both velocity correlation functions decay rapidly to zero and show very little structure. This effect might be attributed to ‘screening’: i. e. each of the particles alters the ambient velocity field, and when these perturbations have a high spatial density and a rapid time dependence, their effect is to produce a strongly

fluctuating background flow which tends to decorrelate the velocity of any particle from its earlier value. An analogous effect is present in porous media flows, which could be thought of as an extreme case of a suspension so concentrated as to be immobile. Here, a static force perturbation in a fluid-saturated porous medium decays exponentially with distance (as seen from the Brinkman equation (Brinkman 1947; Durlofsky & Brady 1987), for example), in contrast to the power-law decay in more dilute mobile suspensions.

In figure 9 we present the time evolution of the average fraction of particles having their initial velocities reversed,

$$n(t) = \left[1 - \left\langle \frac{v_\alpha(0)v_\alpha(t)}{|v_\alpha(0)v_\alpha(t)|} \right\rangle \right] / 2 \quad (4.4)$$

It can be seen that, on average, more than half the particles have both transverse velocity components reversed at intermediate times ($t \sim 1$) for the indicated values of F_0 , r_c and ϕ . These results are consistent with our previous discussion regarding the origin of the negative autocorrelation.

Finally, let us discuss some of the important consequences of the negative correlations in the transverse velocity and their origin. In the first place, it is clear that the integral time scale given by equation (4.2) is different from the autocorrelation time[†]. This is illustrated in figure 10, where we depict the values for τ_{v_y} and τ_{v_z} , obtained using (4.2), as a function of the volume fraction. It is clear that the integral time scale measured from (4.2) fails to capture the actual time scale underlying the loss of correlation in the particle velocities in that it increases with concentration, contrary to the fact that the actual time scale for the correlations becomes shorter as the concentration and the rate of collisions between the particles increases. Also, given the limited accuracy in the

[†] A correlation time defined through equation (4.2) implicitly assumes an exponentially decaying autocorrelation function, as is the case for any Gauss-Markov process (van Kampen 1987, p. 81).

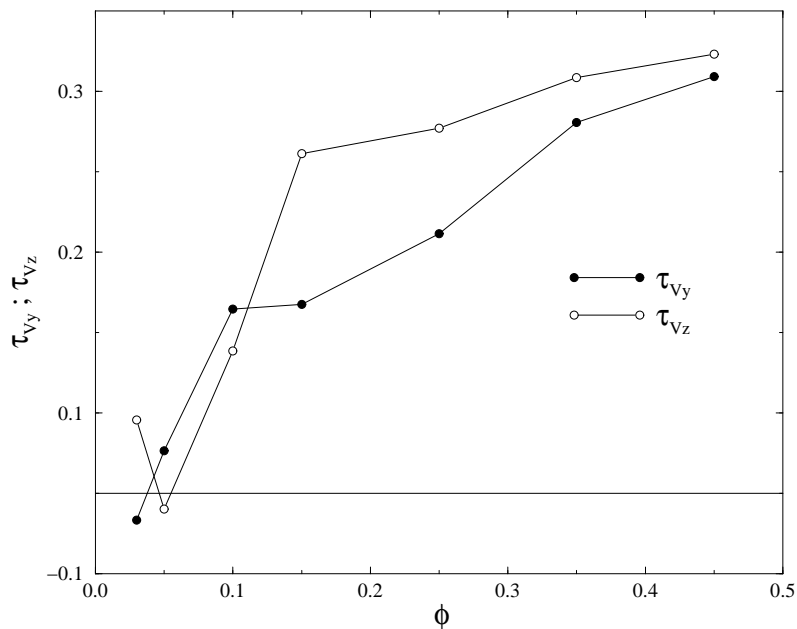


FIGURE 10. τ_{v_y} and τ_{v_z} given by equation (4.2), as a function of the volume fraction. The simulations are for $N = 64$, $N_c = 100$, $F_0 = 1.0$, and $r_c = 10^{-4}$

computation of the integral (4.2), the values of τ_{v_y} and τ_{v_z} shown in figure 10 are subject to large relative errors when $\phi < 0.10$.

The same difficulty is encountered when the diffusion coefficient is evaluated by integrating the velocity autocorrelation function. As previously discussed, the motion generated by binary collisions is not diffusive and thus, in view of equation 4.3, the integral of the autocorrelation function should vanish in the limit $\phi \rightarrow 0$. This is born out by the results shown in figure 10 where it can be seen that the integral of the autocorrelation function approaches zero with decreasing volume fraction. Thus, the leading contribution to the diffusivity comes from a small portion of the autocorrelation function the role of which becomes increasingly more crucial as the volume fraction decreases.

5. Velocity fluctuations

In the previous sections we discussed the loss of correlation in the particle velocities and how the integral time scale is related to the diffusivity. On the other hand, as is clear from equation (4.3), the magnitude of the velocity fluctuations also plays an important role in determining the particle diffusivity. Understanding velocity fluctuations in the presence of long-range hydrodynamic interactions is a long standing problem, and has been recurrently studied in the context of sedimenting suspensions (Brenner & Mucha 2001). In this section we shall present numerical results concerning not only the magnitude of the velocity fluctuations given by σ_v but also the whole probability distribution function (pdf) of the velocity fluctuations, for different volume fractions.

Numerical simulations clearly suffer from two limitations, which become of particular importance when computing velocity fluctuations: the small number of particles in the simulations and the necessary approximations to the hydrodynamic forces (Brady & Bossis 1988). However, we shall show that the functional form of the pdf's undergoes a clear transition, from an exponential to a Gaussian distribution as the volume fraction is increased, which is not sensitive to the number of particles. Moreover, this feature could be measured experimentally thereby providing a useful test for the approximations involved in the hydrodynamic interactions which have been used in constructing the Stokesian dynamics code.

In figure 11 we show the pdf of the velocity fluctuations in the direction of the shear $P(v_y)$, obtained at two different volume fractions, $\phi = 0.05$ and $\phi = 0.35$, and using different number of particles in the simulations. It can be seen that, as previously stated, the distribution of velocities is insensitive to the number of particles, at least as far as its functional form is concerned.

In figure 12 we compare the pdf's at low and high volume fractions in a log-linear

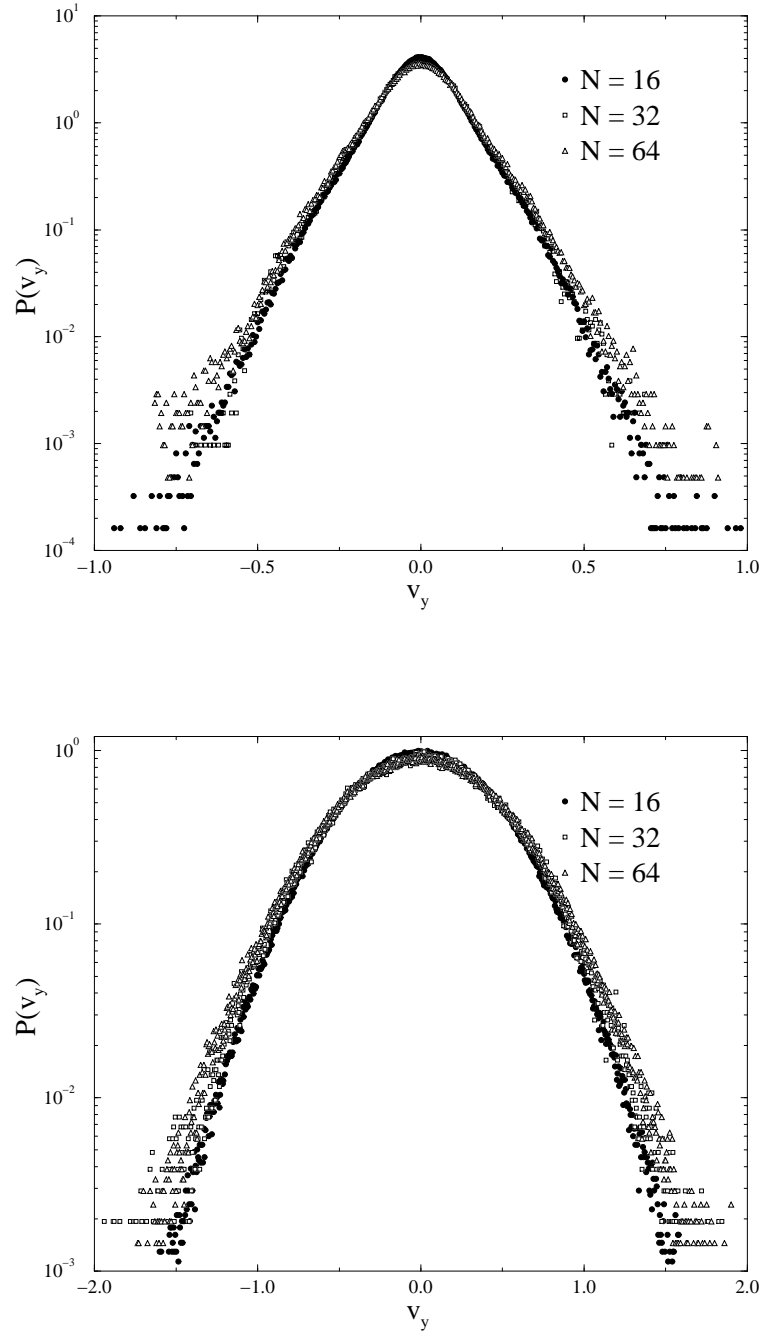


FIGURE 11. Probability density function of the velocity fluctuations in the direction of the shear $P(v_y)$ for two different volume fractions $\phi = 0.05$ and $\phi = 0.35$. Different curves correspond to different number of particles in the numerical simulations. The simulations are for $N = 64$, $N_c = 100$, $F_0 = 1.0$ and $r_c = 10^{-4}$.

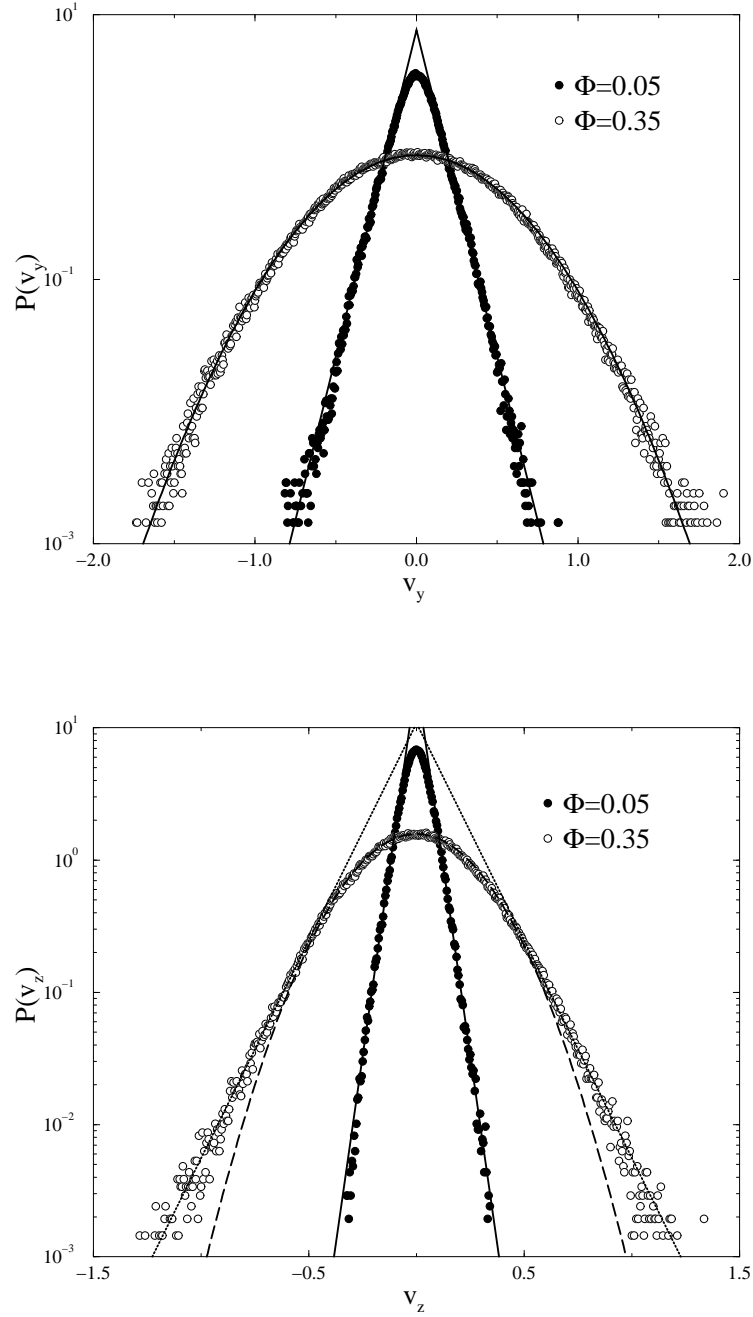


FIGURE 12. Probability density function of the velocity fluctuations in both transverse directions (a) $P(v_y)$ and (b) $P(v_z)$, for two different volume fractions $\phi = 0.05$ and $\phi = 0.35$. See § 5 for a discussion of the different distributions used to fit the numerical data (solid and dashed lines). The simulations are for $N = 64$, $N_c = 100$, $F_0 = 1.0$ and $r_c = 10^{-4}$.

plot. Clearly, both $P(v_y)$ and $P(v_z)$ become not only broader as the concentration increases but change noticeably in their shape. In figure 12a we show that, at low volume fractions ($\phi = 0.05$), $P(v_y)$ is well described by an exponential distribution, $P(v_y) \propto \exp(-11.4 |v_y|)$ but that, at a large volume fraction, $\phi = 0.35$, a Gaussian distribution accurately fits the numerical results, $P(v_y) \propto \exp(-2.41 v_y^2)$. A similar behaviour is observed in $P(v_z)$, as shown in figure 12b in that, at low volume fractions, the pdf is well approximated by an exponential distribution $P(v_z) \propto \exp(-26.3 |v_z|)$, but at large concentrations neither a Gaussian nor an exponential distribution accurately fits the numerical results over the whole range of velocities. However, we show that, for small velocity fluctuations, the distribution is Gaussian (dashed line; $P(v_z) \propto \exp(-7.76 v_z^2)$), whereas large fluctuations are better described by an exponential distribution (dotted line; $P(v_z) \propto \exp(-7.57 |v_z|)$). A similar transition, but in the opposite direction, was observed in fluidized suspensions of non-colloidal particles, where the velocity fluctuation distributions vary from Gaussian to exponential as the particle concentration increases (Rouyer *et al.* 1999, 2000).

We believe that this transition in the pdf of the velocity fluctuations towards a Gaussian distribution, is due to the predominant role played by lubrication forces at the high concentrations. Recall that, given their short-range character, lubrication forces are essentially two-body interactions and are accounted for in a pairwise additive way in the simulation method. On the other hand, again in the simulation method, many-body long-range hydrodynamic interactions are accounted for by means of the far-field approximation[†]. Therefore, the random addition of lubrication forces, generated from spheres

[†] A detailed discussion of the approximations involved in the Stokesian dynamics method can be found elsewhere (Durlofsky *et al.* 1987; Brady & Bossis 1988; Brady *et al.* 1988; Ichiki & Brady 2001).

in close proximity to one another, is the dominant contribution at high concentrations, and would be expected to yield a Gaussian distribution. Let us also note that the hydrodynamic forces inhibit the relative motion of the particles as their approach one another and therefore would prevent large fluctuations in the velocity from occurring, consistent with the range in v_z where a Gaussian distribution properly describes the corresponding pdf's. On the contrary, at low concentrations, lubrication forces becomes negligible and therefore long-range many-body interactions determine the fluctuations in velocity. In this case, our results show an exponential distribution. It is clear then, that a comparison with experimental results would provide another test of the numerical method and of the approximations that are involved in the simulations.

An alternative view of the distinction between Gaussian and exponential velocity distributions may be offered by analogy with turbulence. Specifically, in boundary layer flows, one observes that the pdf of vorticity is Gaussian at low Reynolds numbers, but develops exponential tails at the very high Reynolds numbers characteristic of atmospheric flows (Fan 1991). Similarly (perhaps), the pdf of temperature fluctuations in thermal convection exhibits a transition from Gaussian to exponential as the Rayleigh number increases (Sano *et al.* 1989; Wu 1991). In both cases, the transition is gradual rather than abrupt, and the increase of Reynolds or Rayleigh number is accompanied by the development of organized large-scale coherent structures in the flow (Frisch 1995, p. 100). Since one normally associates Gaussian pdf's with the addition of uncorrelated random variables, it is natural to relate the transition to the more slowly-decaying exponential pdf's to the appearance of correlated long-range structures. In the case of suspensions, inverse concentration is analogous to the Reynolds or Rayleigh number in the sense that a large value of the parameter is associated with long-ranged correlations, as we have seen in the discussion of screening in §4. A common feature in these three situations is that,

at low values of the appropriate control parameter, the motion is relatively uncorrelated and the fluctuations are Gaussian while, at high values, the motion is organized and the fluctuations are more persistent and exponentially distributed.

6. Shear-induced self-diffusion at low concentrations

In section §3 we discussed how stochastic (diffusive-like) transport arises in the deterministic dynamics of sheared suspensions, due to the chaotic evolution in phase space and, in §4, we showed the presence of a stochastic motion at the individual level of a single sphere by studying the loss of correlation in the transverse particle velocities which leads to a random diffusive motion of single particles. Finally, in figure 13, we show that the mean square displacement of a single particle becomes diffusive after a time approximately equal to the characteristic time after which the particle's velocity correlation is lost.

We also discussed the relation between the negative correlation in the transverse velocity fluctuations and the hydrodynamic interaction between a pair of non-Brownian spheres undergoing shear. We also remarked that, in order to get a diffusive motion from purely hydrodynamic interactions, collisions between at least three particles are necessary while, on the contrary, in the presence of non-hydrodynamic forces such as the interparticle repulsive force introduced in §2.1, binary collisions alone lead to diffusive motion. This fact gives rise to different scaling relations for the diffusivity depending on the relative importance of the interparticle force and the hydrodynamic forces. Let the diffusion coefficient in the pure hydrodynamic limit be denoted by D_h , and the contribution to the diffusivity in the presence of non-hydrodynamic forces by D_{n-h} . As already mentioned in §1, since the hydrodynamic contribution D_h arises from collisions between three or more particles, and the rate at which a given sphere interacts with two other spheres is

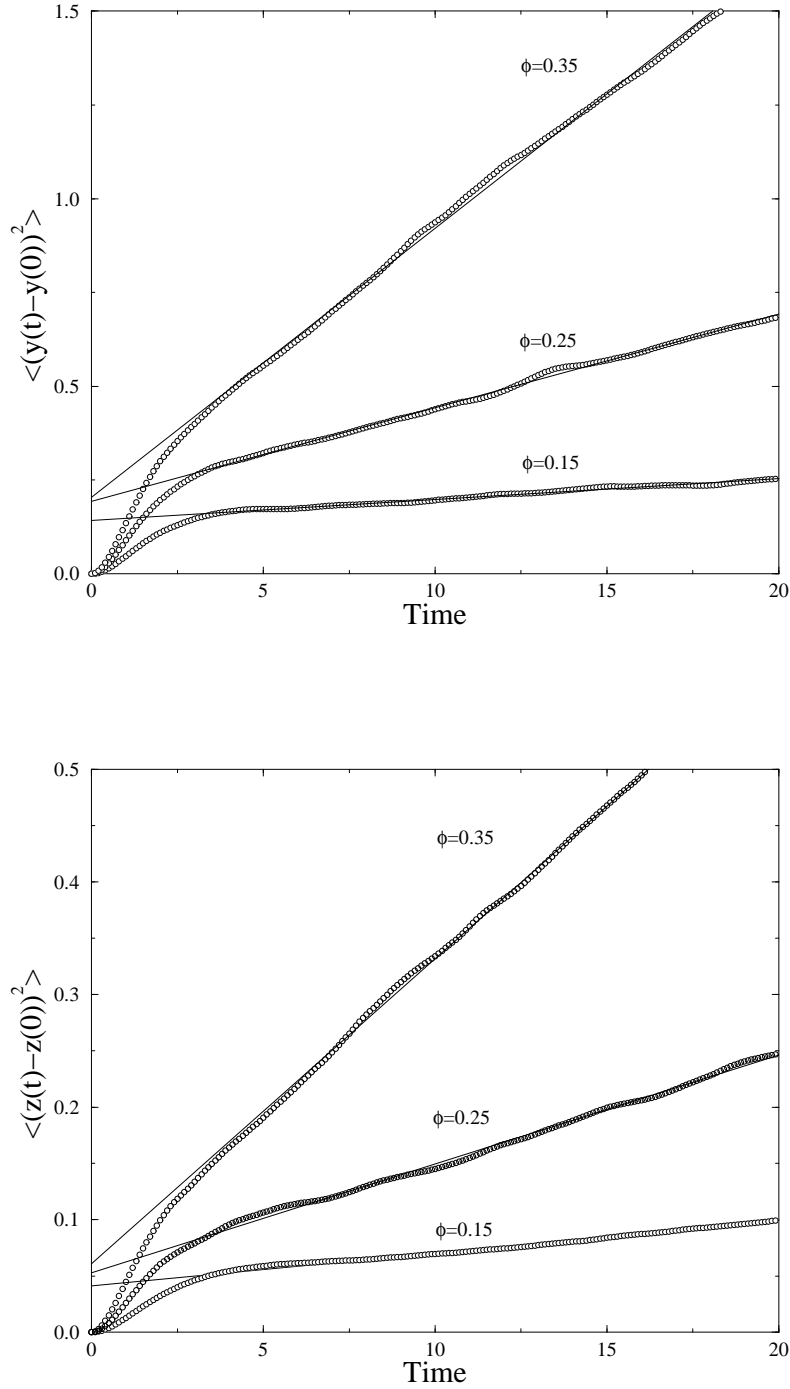


FIGURE 13. Mean square displacement of a single particle, averaged over all the $N = 64$ particles in the suspension and over $N_c = 100$ different realizations, as a function of time for different volume fractions. The magnitude of the interparticle force is $F_0 = 1$ and the characteristic range $r_c = 10^{-4}$.

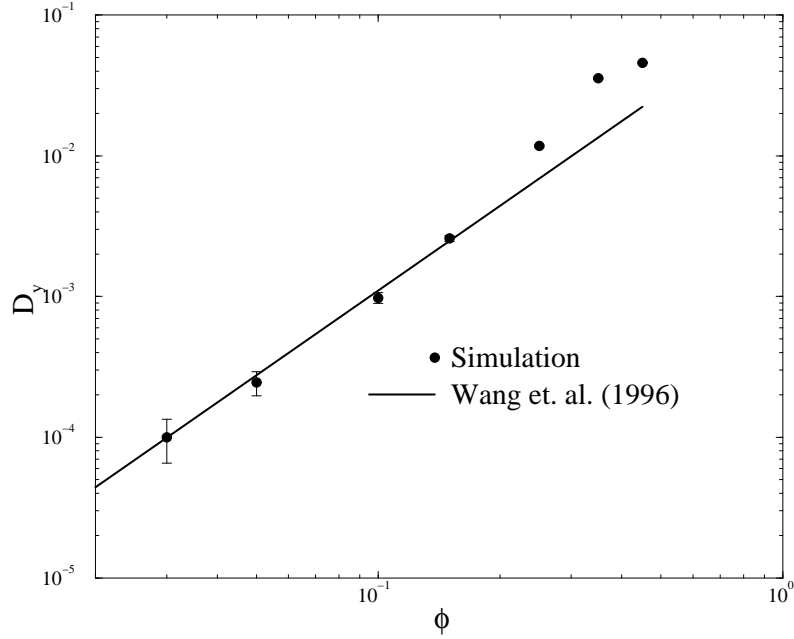


FIGURE 14. Dimensionless diffusion coefficient in the direction of the shear D_y as a function of the volume fraction. The solid line correspond to the theoretical result calculated by Wang *et al.* (1996), in the absence of non-hydrodynamic forces. The simulations are for $N = 64$, $N_c = 100$, $F_0 = 1.0$ and $r_c = 10^{-4}$.

proportional to $\gamma \phi^2$ in the limit of low volume fractions, D_h should scale as $\gamma \phi^2 a^2$ as $\phi \rightarrow 0$ while $D_{n-h} \propto f(F_0, r_c) \gamma \phi a^2$, where $f(F_0, r_c)$ should be an increasing function of the interparticle force magnitude F_0 , and of the range r_c . Then, when interparticle forces are negligible, the diffusion coefficient D will be dominated by the hydrodynamic contribution and should scale as $\gamma \phi^2 a^2$. On the other hand, at low enough concentrations or large interparticle forces, binary collisions become dominant and a linear dependence on the volume fraction should be expected, i. e. $D \sim D_{n-h} \propto \gamma \phi a^2$.

Let us first investigate the case when the interparticle force is negligible. In figure 14 we present, in a log-log plot, D_y the diffusion coefficient in the direction of the shear rendered dimensionless by γa^2 , as a function of the volume fraction where, in all cases,

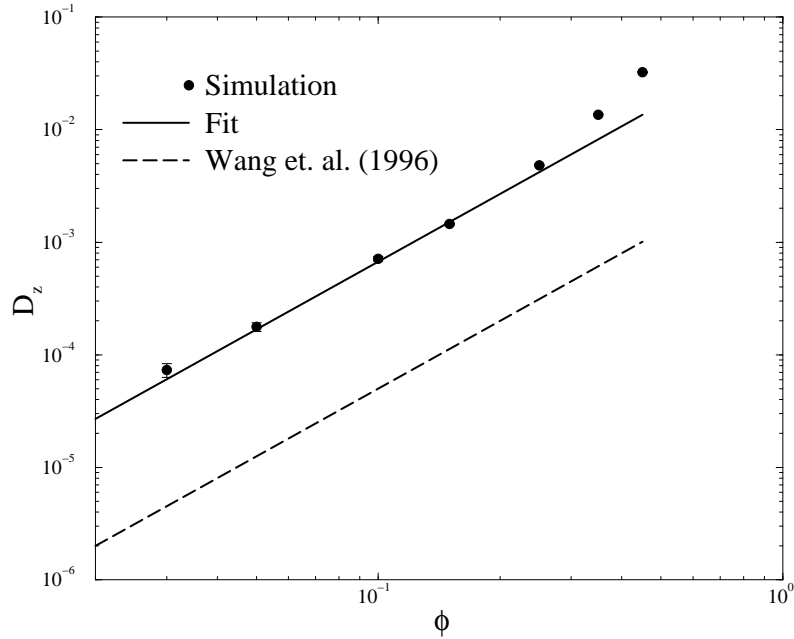


FIGURE 15. Dimensionless diffusion coefficient D_z as a function of the volume fraction. The solid line corresponds to a fit $D_z = 0.07 \phi^2$. The dashed line corresponds to the result obtained by Wang *et al.* (1996), $D_z = 0.005 \phi^2$. The simulations are for $N = 64$, $N_c = 100$, $F_0 = 1.0$ and $r_c = 10^{-4}$.

the diffusion coefficient is obtained from the slope of the mean square displacement in the region of its linear growth, as shown in figure 13. In the numerical simulations the characteristic range of the interparticle force was set to $r_c = 10^{-4}$ and $F_0 = 1.0$. It can be observed that at low volume fractions, a quadratic dependence of D_y on ϕ is obtained, as expected when the non-hydrodynamic force is negligible. We also compare in figure 14 the numerical results with the theoretical values obtained by Wang *et al.* (1996), who evaluated the diffusion coefficient by computing the mean square displacement of a test sphere over all possible encounters with two other spheres in the absence of the non-hydrodynamic force and found that $D_y = 0.11 \phi^2$, in excellent agreement with our fitted value $D_y = (0.11 \pm 0.02) \phi^2$. However, it should be kept in mind that the diffusion

coefficients reported here are from simulations using only 64 particles, a number which may not be large enough for an accurate comparison with other values of D obtained theoretically or experimentally.

In figure 15 we present the dependence of D_z on ϕ . In this case, a quadratic dependence is also found. However, the theoretical values calculated by Wang *et al.* (1996) are much smaller than our numerical results in that a fit to the numerical results gives $D_z = (0.07 \pm 0.007) \phi^2$, whereas Wang *et al.* (1996) found $D_z = 0.005 \phi^2$. However, let us note that the anisotropy found in our simulations for the self-diffusion coefficient, $D_y/D_z \sim 1.5$, is in agreement with the experimental results of Phan & Leighton (1999) recently confirmed by Breedveld *et al.* (2001a).

Let us now consider the case in which the interparticle force contributes significantly to the diffusion coefficient. To this end, we performed simulations with the characteristic range of the interparticle force increased 1000 times relative to its previous value $r_c = 10^{-4}$. The strength of the force was kept constant $F_0 = 1.0$. In figure 16 we present the new numerical results for the diffusion coefficient in the direction of shear, as a function of the volume fraction. For comparison we also show the previous results. It is clear that the diffusivity deviates from the values found previously and becomes larger than before at very low concentrations. As $\phi \rightarrow 0$, a linear dependence on ϕ is found to accurately fit the numerical data, giving $D_y = (7.6 \pm 1.3) \times 10^{-3} \phi$.

In figure 17 the diffusion coefficient in the vorticity plane is compared for the same two values of the characteristic range, $r_c = 10^{-4}$ and $r_c = 10^{-1}$, as a function of ϕ . In this case, the interparticle force is not strong enough and the concentration not low enough for the linear regime to be observed.

It is important to note that the largest range of the interparticle force $r_c = 0.1$ is clearly too large to be considered as representing residual Brownian forces or electro-

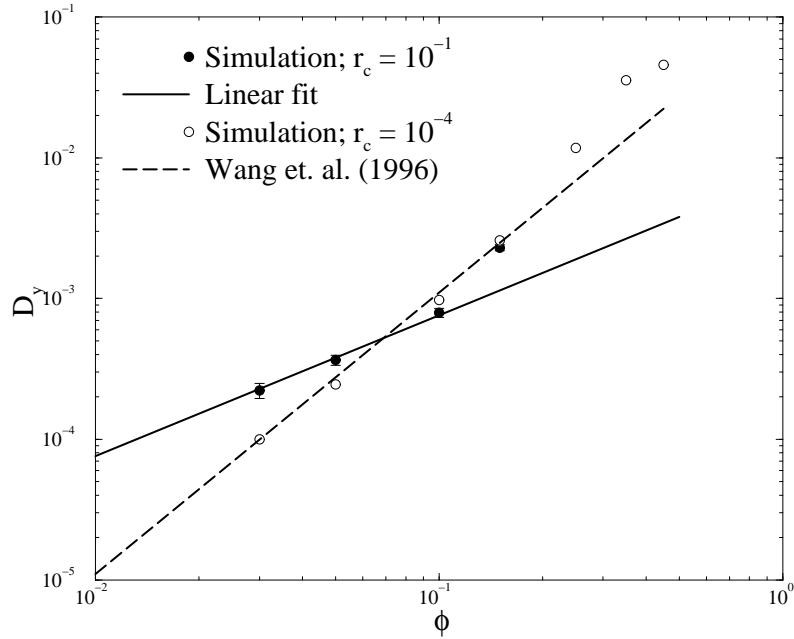


FIGURE 16. Dimensionless diffusion coefficient in the plane of shear D_y as a function of the volume fraction ϕ . Open circles corresponds to short-ranged interparticle forces $r_c = 10^{-4}$, while solid circles correspond to a longer range $r_c = 10^{-1}$. The solid line is a best fit with a linear dependence on ϕ : $D_y = (7.6 \pm 1.3) \times 10^{-3} \phi$. The simulations are for $N = 64$, $N_c = 100$, and $F_0 = 1.0$.

static repulsion (Foss & Brady 2000). However, this force might resemble the effect of particle roughness. By means of numerical simulations, da Cunha & Hinch (1996) and recently Zarraga & Leighton (2001), showed that particle roughness lead to a diffusivity proportional to the volume fraction. These authors modelled particle roughness by a normal force which prevents the particles from coming closer than a minimum dimensionless separation $2 + \epsilon$ between the centres of the two spheres. As a crude approximation, we might estimate the magnitude of the roughness represented by our interparticle force, as its characteristic range r_c , i.e. $\epsilon \sim r_c \sim 0.1$ in our simulations. For $\epsilon \sim 0.1$ da Cunha & Hinch (1996) and Zarraga & Leighton (2001) found that $D_y/\phi \sim 0.02$, which is larger

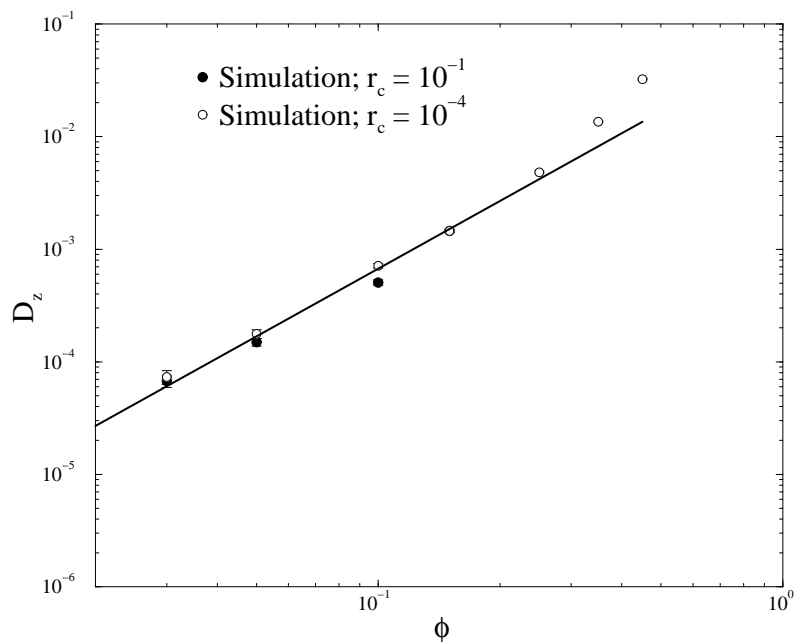


FIGURE 17. Dimensionless diffusion coefficient perpendicular to the plane of shear D_z as a function of the volume fraction ϕ . Open and solid circles corresponds to different characteristic range of the interparticle force, $r_c = 10^{-4}$ and $r_c = 10^{-1}$ respectively. The solid line is the best fit with a quadratic dependence on ϕ , $D_z = (0.07 \pm 0.007) \phi^2$. The simulations are for $N = 64$, $N_c = 100$, and $F_0 = 1.0$.

than our fitted value $D_y/\phi \sim (0.0076 \pm 0.0013)$. However, as shown in figure 18, in our simulations, pairs of particles are allowed to come closer than r_c . This is because, at $r = r_c$ the interparticle force is not infinite as in the analysis by da Cunha & Hinch (1996) and Zarraga & Leighton (2001). On the other hand, if we consider the observed minimum distance between spheres as the effective roughness represented by our repulsive force then, $\epsilon \sim 0.01$ and from da Cunha & Hinch (1996) $D_y/\phi \sim 0.006$, which is now in fairly good agreement with our fitted value. A linear behaviour $D_y \propto \phi$ was also found in experiments by Biemfohr *et al.* (1993) and Zarraga & Leighton (1999). However, the diffusion coefficient reported in these experiments was substantially larger than that

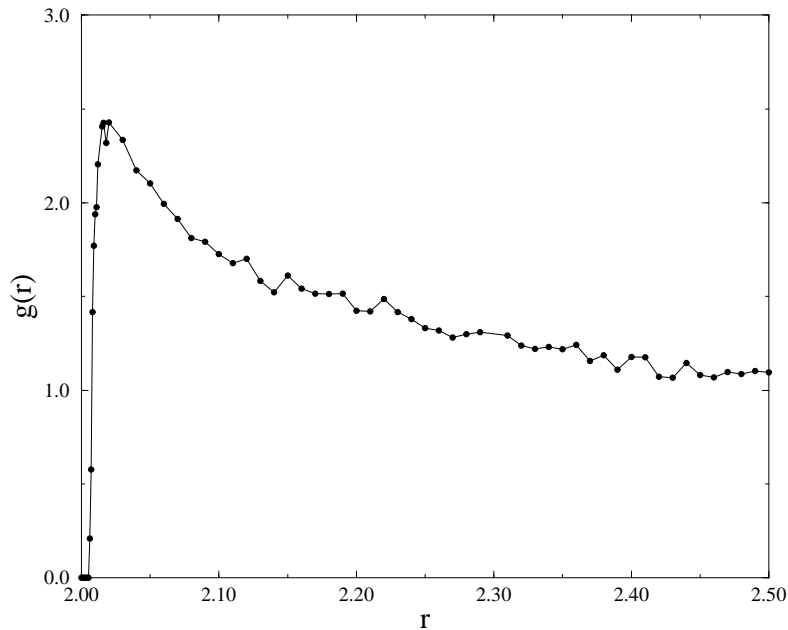


FIGURE 18. Pair distribution function $g(r)$. The characteristic range is $r_c = 0.1$. $N = 64$,
 $\phi = 0.10$, $F_0 = 1.0$, and $N_c = 100$.

obtained by means of numerical simulations ($D_y/\phi \sim 0.03$ as compared to $D_y/\phi \sim 0.005$ from the numerical simulations for $\epsilon \sim 10^{-3}$).

7. Summary

The complex dynamics of homogeneous sheared suspensions of monodisperse, neutrally buoyant, non-Brownian spheres at zero Reynolds number was investigated by means of numerical simulations using Stokesian dynamics. Starting from a large number of independent initial configurations ($N_c = 100$), the evolution of typically $N = 64$ spheres undergoing simple linear shear was simulated during a time $t \sim 100$, which was sufficiently long to allow us to study the dynamics of the system in steady state. In addition to the hydrodynamic interactions between spheres, the simulations included a short-ranged

repulsive interparticle force that qualitatively models the effects of surface roughness and Brownian forces both of which play an important role when neighboring spheres nearly touch one another.

We began by recalling some of the well known effects of the non-hydrodynamic interaction on the microscopic structure of sheared suspensions (Bossis & Brady 1984; Rampall *et al.* 1997). We showed that the location of the first peak of the pair distribution function strongly depends on the range of the interparticle force r_c in that, as r_c is increased, the minimum separation between neighboring spheres increases significantly. We also discussed how the angular distribution of pairs depends on this force, showing that, as the range of the interparticle force is increased, the pair distribution function becomes increasingly more asymmetric, with fewer pairs being oriented downstream than upstream. This asymmetry implies the loss of time reversibility and therefore identifies the interparticle force as a microscopic origin of irreversibility.

The dynamics of sheared suspensions was shown to be chaotic over the whole range of volume fractions investigated, $0.01 < \phi < 0.35$, with the largest Lyapunov exponent increasing linearly with ϕ . The existence of chaos in the dynamics of the suspensions provides an explanation for the loss of correlation in the particle motions leading to diffusive behaviour at long times. In fact, we showed that the system loses memory of its initial state exponentially, and that the asymptotic separation distance between two initially close trajectories in the velocity-space of the two transverse velocity components can be accurately estimated assuming that the two systems are completely uncorrelated.

At the level of individual smooth spheres, we also demonstrate the loss of memory of their instantaneous velocity fluctuations via the transverse velocity autocorrelation function. For high concentration, $\phi \sim 0.40$, a screening-type mechanism is observed and the correlations in particle velocities are lost after a short period of time of $O(1)$. On

the other hand, at the lower concentrations, the transverse particle motions remain, on average, correlated for a longer period of time. We found furthermore that, for both the transverse components of the velocity, the autocorrelation function becomes negative at intermediate times ($t \sim 2$). We proposed an explanation for this effect based in the dynamics of two isolated spheres undergoing simple shear, according to which, since the purely hydrodynamic interaction between two spheres does not lead to any net lateral displacement, it is a source of negative correlation in the velocity fluctuations during binary collisions. This explanation is consistent with the fact that the region within which the velocity autocorrelation function is negative continues to enlarge with decreasing ϕ with the whole autocorrelation function appearing to converge to an asymptotic distribution dominated by binary interactions between spheres. We mentioned that the integral of this asymptotic distribution must vanish on account of its being proportional to the net displacement experienced by a pair of spheres, and showed that, in fact, the numerical value of the integral of the autocorrelation function steadily decreases as $\phi \rightarrow 0$. An important consequence is that the leading contribution to the diffusivity of the particles as $\phi \rightarrow 0$ comes from an asymptotically negligible contribution to the autocorrelation function. Therefore, an estimate of the diffusion coefficient, based on the velocity autocorrelation function, will be highly inaccurate at least for low volume fractions.

At this microscopic level we also computed the velocity probability distribution function in both lateral directions and observed a transition from an exponential to a Gaussian distribution as the volume fraction is increased. We proposed that this transition is due to the dominant role, at high concentrations, of the lubrication forces, which are essentially two-body random interactions and therefore would be expected to give rise to a Gaussian distribution. Unfortunately, there are no experimental measurements thus far of the probability distribution function of the velocity fluctuations.

Finally, we investigated the scaling of the diffusion coefficient D at low concentrations as the range of the interparticle force is varied, by setting D equal to one half the slope of the mean square displacement in the region of its linear growth. For a very small range, $r_c = 10^{-4}$, we showed that the effect of the interparticle force is negligible and D was found to scale as $\gamma\phi^2a^2$ for $0.03 < \phi < 0.15$, both along and normal to the plane of shear. This results corresponds to a diffusive motion arising from collisions between three spheres simultaneously and, in the case of D_y , is in very good agreement with the values obtained by Wang *et al.* (1996), who evaluated the diffusion coefficient by a completely different procedure, viz. by computing the mean square displacement of a test sphere over all possible encounters with two other spheres. On the other hand, for a much larger range of the interparticle force, $r_c = 10^{-1}$, a linear dependence of the diffusion coefficient on ϕ is observed as $\phi \rightarrow 0$, which implies that a significant contribution to the diffusion coefficient emanated from encounters between two particles. This is consistent with the notion that the interparticle force qualitatively mimics the effects of surface roughness and other non-hydrodynamic forces, and reproduces the scaling behaviour found in the theoretical analysis by da Cunha & Hinch (1996) and in the experimental work by Zarraga & Leighton (1999). However, the numerical simulations still fail to reproduce the experimental values of the diffusivity reported by Zarraga & Leighton (1999) by an order of magnitude.

We thank Professor K. Sreenivasan for discussions on the common features between our data and turbulence, and Dr. J. R. Melrose and Professor J. F. Brady for the use of their simulation codes. G. D. thanks M. Tirumkudulu and I. Baryshev for their helpful comments. A.A. and G.D. were partially supported by the National Science Foundation under Grant CTS-9711442 and by the Engineering Research Program, Office of Basic Energy and Sciences, U.S. Department of Energy under Grant DE-FG02-90ER14139; J.K

was partially supported by the Geosciences Research Program, Office of Basic Energy and Sciences, U.S. Department of Energy; G. D. was partially supported by CONICET Argentina and The University of Buenos Aires. Computational facilities were provided by the National Energy Resources Scientific Computer Center.

REFERENCES

- ACRIVOS, A., BATCHELOR, G. K., HINCH, E. J., HOCH, D. L. & MAURI, R. 1992 Longitudinal shear-induced diffusion of spheres in a dilute suspension. *J. Fluid Mech.* **240**, 651–657.
- ALDER, B. J. & WAINWRIGHT, T. 1958 Molecular dynamics by electronic computers. In *Proceedings of the International Symposium on Transport Processes in Statistical Mechanics* (ed. I. Prigogine), pp. 97–131. New York: Interscience publishers.
- ALDER, B. J. & WAINWRIGHT, T. 1967 Velocity autocorrelations for hard spheres. *Phys. Rev. Lett.* **18** (23), 988–990.
- ALDER, B. J. & WAINWRIGHT, T. 1970 Decay of the velocity autocorrelation function. *Phys. Rev. A* **1** (1), 18–21.
- ALLEN, M. P. & TILDESLEY, D. J. 1987 *Computer Simulation of Liquids*. Oxford: Clarendon Press.
- BAKER, G. L. & GOLLUB, J. P. 1990 *Chaotic Dynamics: an introduction*. Cambridge: Cambridge University Press.
- BENETTIN, G., GALGANI, L. & STRELCCYN, J.-M. 1976 Kolmogorov entropy and numerical experiments. *Phys. Rev. A* **14** (6), 2338–2345.
- BIEMFOHR, S., LOOBY, T. & LEIGHTON, D. T. 1993 Measurement of the shear-induced coefficient of self-diffusion in dilute suspensions. In *Proc. DOE/NSF Workshop on Flow of Particles and Fluids*. Ithaca, New York.
- BOSSIS, G. & BRADY, J. F. 1984 Dynamic simulation of sheared suspensions. i. general method. *J. Chem. Phys.* **80** (10), 5141–5161.
- BRADY, J. F. & BOSSIS, G. 1984 Dynamic simulation of sheared suspensions. i. general method. *J. Chem. Phys.* **80** (10), 5141–5152.
- BRADY, J. F. & BOSSIS, G. 1985 The rheology of concentrated suspensions of spheres in simple shear flow by numerical simulation. *J. Fluid Mech.* **155**, 105–129.
- BRADY, J. F. & BOSSIS, G. 1988 Stokesian dynamics. *Annu. Rev. Fluid Mech.* **20**, 111–140.
- BRADY, J. F. & MORRIS, J. F. 1997 Microstructure of strongly sheared suspensions and its impact on rheology and diffusion. *J. Fluid Mech.* **348**, 103–139.

- BRADY, J. F., PHILLIPS, R. J., LESTER, J. C. & BOSSIS, G. 1988 Dynamic simulation of hydrodynamically interacting suspensions. *J. Fluid Mech.* **195**, 257–280.
- BREEDVELD, V., VAN DEN ENDE, D., BOSSCHER, M. B., LOMGSCHAAP, J. J. J. & MELLENA, J. 2001*a* Measuring shear-induced self-diffusion in a counterrotating geometry. *Phys. Rev. E* **63**, 021403.
- BREEDVELD, V., VAN DEN ENDE, D., LOMGSCHAAP, J. J. J. & MELLENA, J. 2001*b* Shear-induced diffusion and rheology of noncolloidal suspensions: Timescales and particle displacements. *J. Chem. Phys.* **114**, 5923–5936.
- BREEDVELD, V., VAN DEN ENDE, D., TRIPATHI, A. & ACRIVOS, A. 1998 The measurement of the shear-induced particle and fluid tracer diffusivities in concentrated suspensions by a novel method. *J. Fluid Mech.* **375**, 297–318.
- BRENNER, M. P. & MUCHA, P. J. 2001 That sinking feeling. *Nature* **409**, 568–570.
- BRINKMAN, H. C. 1947 A calculation of the viscous force exerted by a flowing fluid on a dense swarm of particles. *Appl. Sci. Res.* **A** (1), 27–34.
- DA CUNHA, F. R. & HINCH, E. J. 1996 Shear-induced dispersion in a dilute suspension of rough spheres. *J. Fluid Mech.* **309**, 211–223.
- DORFMAN, J. R. 1998 Deterministic chaos and the foundations of the kinetic theory of gases. *Phys. Rep.* **301**, 151–185.
- DRATLER, D. I. & SCHOWALTER, W. R. 1996 Dynamic simulation of suspensions of non-brownian hard spheres. *J. Fluid Mech.* **325**, 53–77.
- DURLOFSKY, L. & BRADY, J. F. 1987 Analysis of the brinkman equation as a model for flow in porous media. *Phys. Fluids* **30** (11), 3329–3341.
- DURLOFSKY, L., BRADY, J. F. & BOSSIS, G. 1987 Dynamic simulation of hydrodynamically interacting particles. *J. Fluid Mech.* **180**, 21–49.
- ECKMANN, J. P. & RUELLE, D. 1985 Ergodic theory of chaos and strange attractors. *Rev. Mod. Phys.* **57** (3), 617–656.
- ECKSTEIN, E. C., BAILEY, D. G. & SHAPIRO, A. H. 1977 Self-diffusion of particles in shear flow of a suspension. *J. Fluid Mech.* **79** (1), 191–208.
- FAN, M. S. 1991 Features of vorticity in fully turbulent flows. PhD thesis, Yale University.

- FOSS, D. R. & BRADY, J. F. 2000 Structure, diffusion and rheology of brownian suspensions by stokesian dynamics simulation. *J. Fluid Mech.* **407**, 167–200.
- FRISCH, U. 1995 *Turbulence: the legacy of A. N. Kolmogorov*. Cambridge: Cambridge University Press.
- GADALA-MARIA, F. & ACRIVOS, A. 1980 Sheared-induced structure in a concentrated suspension of solid spheres. *J. Rheology* **24**, 799–814.
- GASPARD, P. 1998 *Chaos, scattering and statistical mechanics*. New York: Cambridge University Press.
- ICHIKI, K. & BRADY, J. F. 2001 Many-body effects and matrix inversion in low-reynolds-number hydrodynamics. *Phys. Fluids* **13** (1), 350–353.
- VAN KAMPEN, N. G. 1987 *Stochastic Processes in Physics and Chemistry*. Amsterdam: North-Holland.
- LEAL, L. G. 1992 *Laminar Flow and Convective Transport Processes*. Boston: Butterworth-Heinemann.
- LEIGHTON, D. & ACRIVOS, A. 1987 Measurement of shear-induced self-diffusion in concentrated suspensions of spheres. *J. Fluid Mech.* **177**, 109–131.
- MARCHIORO, M. & ACRIVOS, A. 2001 Shear-induced particle diffusivities from numerical simulations. *J. Fluid Mech.* To appear.
- NICOLAI, H., HERZHAFT, B., HINCH, E. J., ONGER, L. & GUZZELLI, E. 1995 Particle velocity fluctuations and hydrodynamic self-diffusion of sedimenting non-brownian spheres. *Phys. Fluids* **7** (1), 12–23.
- PARISI, F. & GADALA-MARIA, F. 1987 Fore-and-aft asymmetry in a concentrated suspension of solid spheres. *J. Rheol.* **31** (8), 725–732.
- PHAN, S. E. & LEIGHTON, D. T. 1999 Measurement of the shear-induced tracer diffusivity in concentrated suspensions. *J. Fluid Mech.* Submitted.
- RAHMAN, A. 1964 Correlations in the motion of atoms in liquid argon. *Phys. Rev.* **136** (2A), 405–411.
- RAMPALL, I., SMART, J. R. & LEIGHTON, D. T. 1997 The influence of surface roughness on the

- particle-pair distribution function of dilute suspensions of non-colloidal spheres in simple shear flow. *J. Fluid Mech.* **339**, 1–24.
- ROUYER, F., LHUILIER, D., MARTIN, J. & SALIN, D. 2000 Structure, density, and velocity fluctuations in quasi-two-dimensional non-brownian suspensions of spheres. *Phys. Fluids* **12** (5), 958–963.
- ROUYER, F., MARTIN, J. & SALIN, D. 1999 Non-gaussian dynamics in quasi-2d noncolloidal suspension. *Phys. Rev. Lett.* **83** (5), 1058–1061.
- SANO, M., WU, X. Z. & LIBCHABER, A. 1989 Turbulence in helium-gas free convection. *Phys. Rev. A* **40** (11), 6421–6430.
- SCHUSTER, H. G. 1989 *Deterministic chaos*. Weinheim: VCH.
- WANG, Y., MAURI, R. & ACRIVOS, A. 1996 The transverse shear-induced liquid and particle tracer diffusivities of a dilute suspension of spheres undergoing a simple shear flow. *J. Fluid Mech.* **327**, 255–272.
- WANG, Y., MAURI, R. & ACRIVOS, A. 1998 Transverse shear-induced gradient diffusion in a dilute suspension of spheres. *J. Fluid Mech.* **357**, 279–287.
- WU, X. Z. 1991 Along a road to developed turbulence: free thermal convection in low temperature helium gas. PhD thesis, Chicago University.
- ZARRAGA, I. E. & LEIGHTON, D. T. 1999 Anomalous diffusion in a dilute suspension of non-colloidal spheres. Unpublished.
- ZARRAGA, I. E. & LEIGHTON, D. T. 2001 Normal stress and diffusion in a dilute suspension of hard spheres undergoing simple shear. *Phys. Fluids* **13** (3), 565–577.